Laser cleaning of diagnostic mirrors from tungsten–oxygen tokamak-like contaminants

2016 Nucl. Fusion 56 086008

(http://iopscience.iop.org/0029-5515/56/8/086008)

OPEN ACCESS
IOP Publishing | International Atomic Energy Agency
Nuclear Fusion
Nucl. Fusion **56** (2016) 086008 (9pp)
doi:10.1088/0029-5515/56/8/086008

Laser cleaning of diagnostic mirrors from tungsten–oxygen tokamak-like contaminants

A. Maffini[1], A. Uccello[2], D. Dellasega[1,2] and M. Passoni[1,2]

[1] Dipartimento di Energia, Politecnico di Milano, Italy
[2] Istituto di Fisica del Plasma 'Piero Caldirola', Consiglio Nazionale delle Ricerche, IFP-CNR, Milan, Italy

E-mail: alessandro.maffini@polimi.it

Received 2 March 2016, revised 9 May 2016
Accepted for publication 6 June 2016
Published 14 July 2016

Abstract

This paper presents a laboratory-scale experimental investigation about the laser cleaning of diagnostic first mirrors from tokamak-like contaminants, made of oxidized tungsten compounds with different properties and morphology. The re-deposition of contaminants sputtered from a tokamak first wall onto first mirrors' surfaces could dramatically decrease their reflectivity in an unacceptable way for the proper functioning of plasma diagnostic systems. The laser cleaning technique has been proposed as a solution to tackle this issue. In this work, pulsed laser deposition was exploited to produce rhodium films functional as first mirrors and to deposit onto them contaminants designed to be realistic in reproducing materials expected to be re-deposited on first mirrors in a tokamak environment. The same laser system was also used to perform laser cleaning experiments, exploiting a sample handling procedure that allows one to clean some cm^2 in a few minutes. Cleaning effectiveness was evaluated in terms of specular reflectance recovery and mirror surface integrity. The effect of different laser wavelengths ($\lambda = 1064$, 266 nm) on the cleaning process was also addressed, as well as the impact of multiple contamination/cleaning cycles on the process outcome. A satisfactory recovery of pristine mirror reflectance ($\geqslant 90\%$) was obtained in the vis–NIR spectral range, avoiding at the same time mirror damaging. The results here presented show the potential of the laser cleaning technique as an attractive solution for the cleaning of diagnostic first mirrors.

Keywords: laser cleaning, first mirrors, tokamak, pulsed laser deposition, rhodium, tungsten

(Some figures may appear in colour only in the online journal)

1. Introduction

Metallic first mirrors (FMs) will be crucial components of all optical systems for plasma diagnostics and imaging tools in ITER [1, 2]. They must survive a harsh environment consisting of intense thermal loads, strong radiation fields and high particle fluxes. The two main effects of these extreme conditions are erosion due to interactions with plasma ions and charge exchange neutrals and re-deposition of sputtered material—such as beryllium (Be) and tungsten (W) compounds—transported from the first wall to the mirror surface. In particular, the latter can lead to a dramatic decrease of FM specular reflectance, affecting the performance of the corresponding diagnostic systems with an ultimate impact on reactor safety and operations [2–5]. It is difficult to predict the exact nature of the re-deposited contaminant, whose elemental, chemical and morphological characteristics depend on a number of factors, primarily the specific features of the tokamak first wall.

Experimental campaigns devoted to the investigation of material migration and deposition onto test mirrors have been carried out in tokamaks with metallic first walls, like ASDEX Upgrade (AUG) [4] and the JET ITER-Like Wall (JET-ILW) [5]. Copper and molybdenum (Mo) mirrors were installed in AUG (under the divertor dome, on the upper baffle area and in a remote region at the entrance of a pump duct) and exposed for the entire 2010–2011 AUG campaign [4]. The reflectance of all the exposed mirrors degraded due to impurity deposition (mainly of tungsten trioxide, WO_3, and boron), especially in the UV–vis spectral region. The most severe reflectivity drop ($\sim$55%) was experienced by the mirror placed under the dome, which was covered by a bluish, 70 nm thick WO_3 coating [4]. In JET, a thorough FM test experiment was performed exposing several molybdenum mirrors to JET-ILW plasma. All the mirrors from the divertor zone lost reflectance (by 50%–85%) due to Be, carbon (C), nitrogen, oxygen (O) and W co-deposition [5]. They were covered by smooth colourful layers, having thickness varying from tens of nanometers up to 600 nm [5]. In this case, W was only a fraction of the deposited layer (W/Be $\sim$ 10 at.% for mirrors in the divertor base), whose composition was dominated by Be and O. Nevertheless, the W content sharply increased with increasing heating power in JET operation [5], so one can expect that deposits with a significant fraction of W will not be unlikely in ITER.

The severe reflectance degradation suffered by contaminated mirrors motivates research efforts currently devoted to coping with the problem of re-deposition, both in terms of mitigation strategies (such as shutters, gas blows in front of FMs, introduction of special diagnostic duct geometries, etc) and *in situ* cleaning techniques. Today, the most studied techniques are plasma cleaning [6–9] and laser cleaning [10–14].

Preliminary experiments have been performed to laser-clean test mirrors retrieved from JET [10, 14] and HL-2A [11]. Despite some promising results, these works have highlighted some peculiar issues that should be addressed. Firstly, a partial removal of contaminants—potentially sufficient to guarantee the proper operation of other plasma-facing components—may not be enough to recover the optical properties of the FMs. Secondly, the imperative need to avoid any damage to the mirror surface—also for repeated cycles of cleaning—limits the range of allowed laser parameters (wavelength, fluence per pulse, number of of pulses per site), influencing therefore the overall cleaning efficacy. On the one hand, a careful optimization of the laser parameters is thus mandatory; on the other hand the complex physics inherent to the laser cleaning process makes the choice of cleaning parameters strongly dependent on mirror and contaminant characteristics. A systematic investigation is therefore needed to assess the laser cleaning technique as a solution for FM recovery in a fusion machine.

The limited availability of test mirrors exposed in tokamaks, exacerbated by the burden of working with toxic Be and possibly tritium contamination, hinders such a methodical investigation only relying on mirrors contaminated in a tokamak environment. A complementary approach is to simulate at the laboratory scale the process of contaminant re-deposition which occurs in tokamaks, using suitable deposition techniques. Indeed, the ability to obtain ad hoc artificially contaminated mirrors can be exploited to determine the best process parameters as a function of the contaminant characteristics (composition, morphology, thickness, micro- and nanostructure, etc). The usefulness of this strategy becomes even more evident considering that the exact nature of re-deposition phenomena in ITER is unknown, and so the ability to prove the robustness of the technique against different kinds of contaminants is particularly valuable. Moreover, a lab-scale approach is clearly necessary to study the effects of multiple contamination/cleaning cycles, a task that would require years if performed by exposing mirrors in present-day tokamaks.

This paper aims to provide a thorough laboratory-scale investigation about the laser cleaning of diagnostic FMs from W–O contamination, in conditions potentially relevant to ITER. In our previous works [15, 16] we developed a novel strategy for the study of the laser cleaning of FMs in lab facilities. In particular, the same Nd:YAG nanosecond laser source is exploited for three purposes: (i) production of rhodium (Rh) mirrors realistic as FM coatings [17, 18], (ii) deposition of properly designed contaminants onto mirrors' surfaces and (iii) laser cleaning of contaminated mirrors.

Rh has been chosen because it is one of the principal candidate materials for the development of FMs in ITER [19]. As a first step toward ITER-relevant materials, in previous works we studied the cleaning of C contaminants [15, 16]. Here, the investigation is extended to tungsten–oxygen (W–O) compounds, as oxidized re-deposits were observed in tokamaks operating with a metal wall [4, 5, 20]. The versatility of the pulsed laser deposition (PLD) technique allowed us to produce contaminants with different morphology (compact films versus porous foam-like deposits), thickness (from 100 nm up to 1 μm) and O content.

The results of laser cleaning experiments were mainly evaluated by reflectance measurements, together with the mirrors' surface characterization before and after the cleaning process. To preliminary assess the feasibility of the laser cleaning technique in an operative environment, we also addressed the effect of repeated contamination–cleaning cycles.

The experimental set-up and the features of the mirrors employed in the cleaning experiments are described in section 2. The process of W-based contaminant production is detailed in section 3. The laser cleaning procedure is presented in section 4, and the cleaning results are discussed in section 5. Concluding remarks are given in section 6.

2. Experimental set-up and mirror production

Our PLD apparatus exploits a Q-switched Nd:YAG laser with a tunable wavelength (λ = 1064, 532 and 266 nm), pulse duration of 5–7 ns and a repetition rate of 10 Hz. The laser beam has a circular shape of $\varnothing$ = 9 mm, and it can be focused onto the sample thanks to a converging lens. The laser pulses hit a target made of the material to be deposited at 45°, causing the evaporation of its superficial layers. The ablated species expand in a high-vacuum chamber (base pressure 10^{-3} Pa) that can be filled with inert or reactive gases at a desired pressure, and finally impinge on a suitable substrate placed at a distance d_{T-S} from the target.

The samples were characterized, before and after laser cleaning, with a Zeiss Supra 40 field emission scanning electron microscope (SEM, accelerating voltage 3–7 kV) to assess their surface morphology. Deposit composition was checked with energy-dispersive X-ray spectroscopy (EDXS) using an accelerating voltage of 5 kV to excite the core electronic transitions of W ($M_\alpha = 1.77$ keV) and O ($K_\alpha = 0.52$ keV). A Renishaw inVia Raman spectrometer using the 514.5 nm wavelength of an argon (Ar) laser was exploited to determine the chemical and structural properties of the samples. In addition, the specular reflectance (R_{spec}) of the Rh mirrors (before contamination, after contamination and after cleaning) was determined subtracting the diffuse reflectance (R_{diff}) from the total reflectance (R_{tot}), both measured by a UV–vis–NIR PerkinElmer Lambda 1050 spectrophotometer with a 150 mm Spectralon integrating sphere in the 250–1800 nm wavelength range, of interest for most ITER diagnostics [1].

The process of ITER-like Rh mirror production by PLD is described in detail in [17, 18]. Among the possible nanostructures obtainable by means of PLD, the highly-oriented polycrystalline one (preferential growth direction (1 1 1)) was chosen, mainly because of its high adhesion to the substrate which could guarantee a higher laser damage threshold [15]. Two kinds of substrates were employed: (1 0 0) silicon (Si) wafer and mirror-polished P-91 steel substrates. In both cases the mirror size was 2.6×2.6 cm^2. Rh coatings were uniform on the whole area, with a thickness of $\approx 1 \pm 0.1$ μm.

3. W–O contaminant production

Two peculiar W–O morphologies were produced by means of PLD: compact films and porous foam-like deposits. These two morphologies can be regarded as representative of the wide variety of materials that can possibly re-deposit on FMs. Compact W–O films were modelled upon deposits found on mirrors exposed in AUG [4]. Porous W–O contaminants morphologically resemble the sponge-like W re-deposits found in AUG on the outer divertor strike point tiles [21] and the fuzzy W structure formed on plasma exposure in linear devices [22, 23].

A 99.9% purity tungsten target was ablated by laser pulses with $\lambda = 532$ nm. The laser fluence per pulse on the target was 2.2 J cm^{-2}. By means of an O_2 or Ar atmosphere it was possible to tune the energy of the W species impinging the Rh film, and—in the case of O_2—promote oxidation reactions in the ablation plume. All depositions were carried out at room temperature, and d_{T-S} was kept fixed at 6 cm.

Compact W–O films were obtained using 5 Pa of O_2 as the background atmosphere. At visual inspection, the compact W–O coatings deposited on Rh presented a relatively uniform blue-green colour, similar to the deposit found on the Mo mirror exposed in AUG under the divertor dome [4] (see figure 1.) From the SEM investigation, the films' surfaces appeared smooth and featureless (not shown). The films' thicknesseses were approximately 100 nm. EDXS analysis showed an O/W atomic ratio ~2.8, close to that of WO_3.

A typical Raman spectrum of a compact W–O sample is shown in figure 2 (black line). It presents two broad bands in

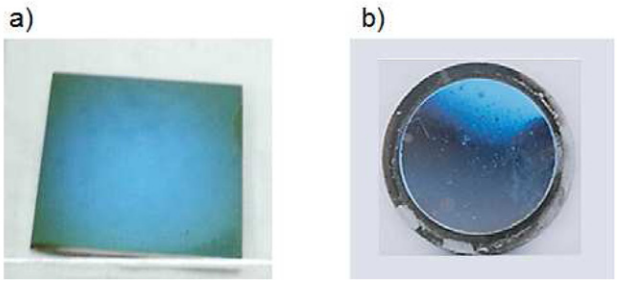

Figure 1. (*a*) Photograph of a Rh mirror contaminated with pulsed laser deposited compact W–O. (*b*) Photograph of a molybdenum mirror after exposure in AUG. Reprinted with permission from [4]. Copyright 2013 IAEA.

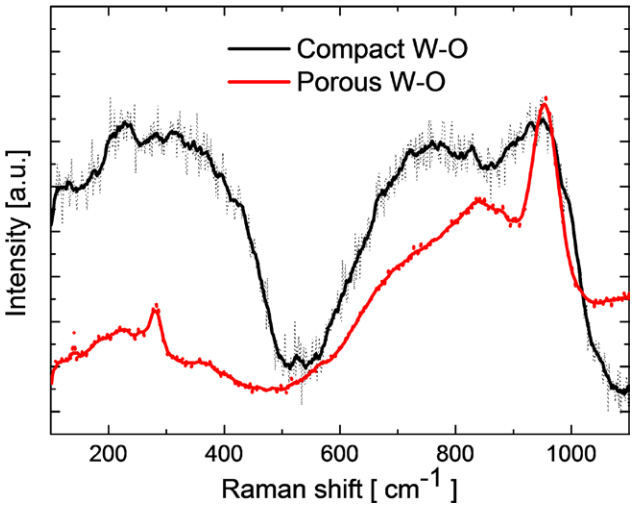

Figure 2. Intensity normalized Raman spectra of compact W–O deposited with 5 Pa O_2 (black line) and porous W–O deposited with 100 Pa Ar (red line).

the 100–500 cm^{-1} (associated with O–W–O bending modes) and 600–1000 cm^{-1} (associated with W–O stretching modes) regions. One can trace the origin of these bands back to the peaks of crystalline WO_3, which are broadened by the lack of crystalline order typical of amorphous oxides.

Porous W–O deposits were obtained with 100 Pa of Ar as the background atmosphere. In this condition, the kinetic energy of the ablated species impinging on the substrate is greatly decreased by the scattering with the Ar atoms. The resulting reduced adatom mobility is responsible for the foam-like morphology of these deposits. The morphologies of PLD porous W–O deposits, sponge-like W re-deposits found in AUG [21], and fuzzy W nanostructures [23] are compared in figure 3. Porous W–O deposits produced by PLD (figures 3(*a*) and (*b*)) and fuzzy W nanostructures (figure 3(*d*)) are characterized by the presence of nanometric filaments and micrometric voids. The porosity of sponge-like W re-deposits (figure 3(*c*)) is in the nanometer-scale range.

Even though the porous W–O contaminants were deposited in an inert atmosphere, the O/W atomic ratio as determined by EDXS was ~2.6. Probably the high surface-to-volume ratio of this foam-like nanostructure led to an enhanced spontaneous surface oxidation when the deposits were exposed to ambient air. The Raman spectra of the porous W–O deposits (figure 2, red line) are

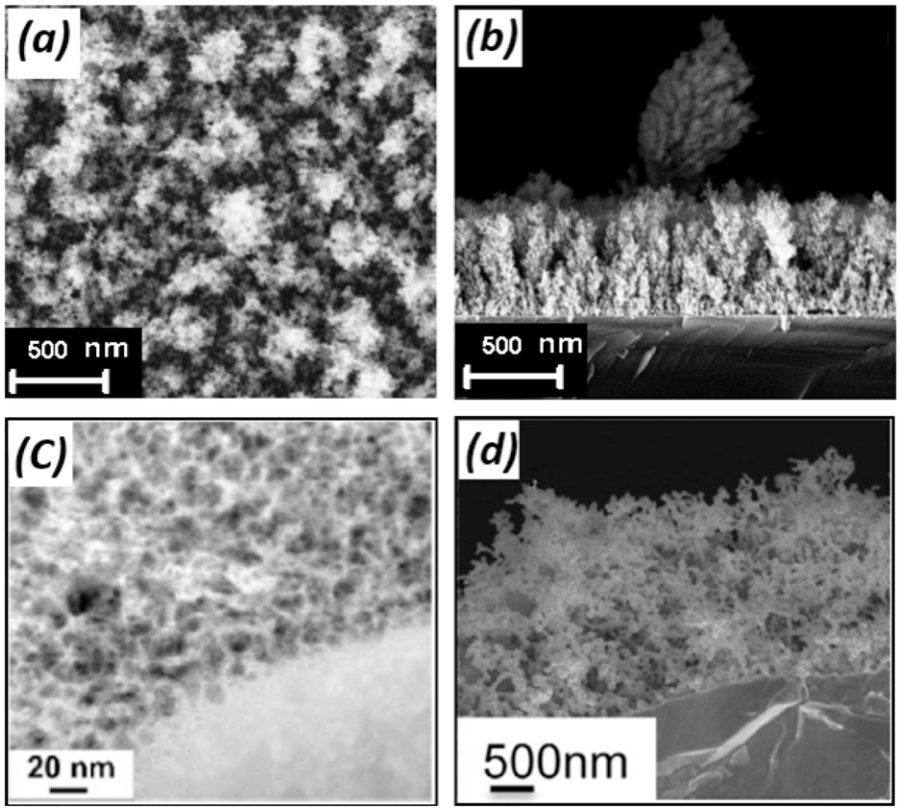

Figure 3. (*a*) SEM plane view and (*b*) cross-section view of a PLD porous W–O deposit (average thickness ∼600 nm). (*c*) STEM *Z*-contrast cross-section image of the material re-deposited in the outer divertor region of AUG (reprinted with permission from [21]; copyright 2011 Elsevier). (*d*) Morphology of W surface exposed to low-energy helium plasma for 500 s at a fixed temperature of 1000 °C (reprinted with permission from [23]; copyright 2012 AIP Publishing).

dominated by a strong peak at 960 cm^{-1}, which does not have any correspondence to the Raman peaks of crystalline WO_3. In the literature, this peak has been attributed to the stretching mode of W = O double bonds that are present on the surface of the nano-cluster and void structures [24, 25]. The intense 960 cm^{-1} feature therefore confirms the high degree of nanostructuration and the high surface-to-volume ratio of the porous W–O deposits [24].

The typical total and diffuse reflectance spectra for the W–O contaminated mirrors are shown in figures 4(*a*) and (*b*), respectively. The R_{tot} of the mirror contaminated with compact W–O (line II, dotted red) oscillates between ∼0% and ∼50%, with two minima and maxima clearly visible. The same oscillating behaviour characterizes its R_{diff}, which ranges from ∼0% to ∼7%. The R_{tot} of the mirror contaminated with porous W–O (line III, dashed blue) is high (⩾60%) for $\lambda > 600$ nm, and then smoothly goes to ∼0% as the wavelength decreases. Conversely, its R_{diff} presents a right skewed peak around 400 nm (peak value ∼20%). The optical properties of the contaminated mirrors are mainly influenced by two contributions: inter-band light absorption in the contaminant (the bulk WO_3 band gap is around 2.8 eV) and surface morphological effects (diffuse scattering and thin-film interference). It is known that the fraction of light scattered outside the specular angle (i.e. R_{diff}) increases exponentially with the square of the ratio between the surface roughness and the light wavelength [26].

The R_{tot} of the mirrors contaminated with compact W–O (figure 4(*a*), II, dotted red line) can be thought of as the convolution between the thin-film interference pattern (responsible for the wavy feature) and the inter-band photon absorption for $\lambda < 450$ nm (which corresponds to a photon energy >2.75 eV). The same mirrors presented a relatively low R_{diff} (figure 4(*b*), II, dotted red line) because of their smooth and regular surfaces.

Porous W–O deposits do not show interference fringes because they do not have a well-defined, flat surface. Therefore the reflectance decrease due to inter-band absorption appears clearly in the near-UV region (figure 4(*a*), III, blue line). On the other hand R_{diff} (figure 4(*b*), III, blue line) increases as the wavelength decreases because of diffuse scattering, and then sharply falls to 0% when inter-band photon absorption becomes dominant.

In general, the optical properties of the mirrors after the deposition of PLD W–O contaminants are similar to those of mirrors retrieved from AUG after plasma exposure, characterized by a marked reflectance decrease in the UV–vis wavelength region (see figure 4 in [4]).

The results here reported show the PLD capability of mimicking different kinds of fusion-relevant deposits, in terms of material composition, morphology, and optical properties.

4. Laser cleaning procedure and process parameters

In the laser cleaning experiments, the PLD apparatus was modified by replacing the target with the sample to be cleaned.

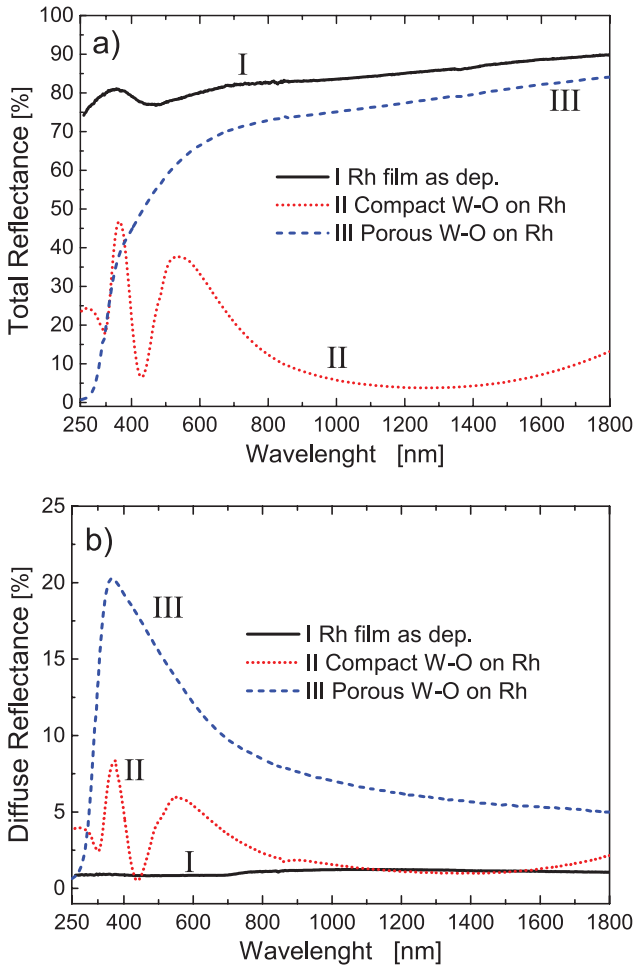

Figure 4. (*a*) R_{tot} and (*b*) R_{diff} of a Rh mirror before contamination (I, solid black), after contamination with compact W–O (II, dotted red) and after contamination with porous W–O (III, dashed blue).

Laser cleaning was performed in high vacuum (3×10^{-3} Pa) [16]. The laser beam hit the sample at 45°, and the laser spot on the sample had an elliptical shape with a major axis of ∼13 mm and a minor axis of ∼9 mm. With the aim of cleaning areas of some cm^2 to ensure the uniform irradiation of the sample, the latter was moved during the cleaning. In [16], we described a sample handling procedure that allows fast and uniform irradiation and is readily scalable to samples of larger size.

The sample to be cleaned was vertically moved with velocity v_y. The laser pulses thus described a vertical stripe on the sample surface. Once the laser spot had travelled the entire vertical length of the sample, the irradiation was suspended and the sample was moved laterally by a predefined step Δx. Then, another vertical stripe—this time in the opposite way—was performed. These steps can be repeated until all of the sample surface is irradiated: the completion of the whole procedure is defined hereafter as a *scan*. Choosing $\Delta x = 6$ mm and $v_y = 4\,\text{mm s}^{-1}$ each point of the sample received approximately 45 pulses per scan, and the time required to clean a 2.6×2.6 cm^2 mirror was around 1 min. This choice proved to be a good compromise among cleaning effectiveness, time requirement and substrate integrity [16]. Multiple scans can be repeated on the same sample if required; in order to mitigate the effects of possible laser non-uniformity, the sample holder was rotated by 90° between one scan and another.

We initially considered two laser wavelengths: $\lambda = 1064$ nm (NIR) and $\lambda = 266$ nm (UV). The laser fluence (defined as the energy per pulse divided by the laser beam size) for each wavelength must be chosen according to the strict requirement of leaving the mirror's surface undamaged during the laser cleaning treatment. In [15] and [16], we found that the damage threshold for bare highly-oriented Rh coatings deposited on Si was higher than 350 mJ cm^{-2} for NIR and 150 mJ cm^{-2} for UV pulses, using the irradiation procedure described above. Due to some concerns about the stability of the laser system during UV operation, the laser fluence for the UV cleaning trials described hereafter was set to 110 mJ cm^{-2}.

As a first step, the preliminary cleaning experiments were devoted to investigating the effect of the laser wavelength on cleaning effectiveness. Two mirrors, contaminated with compact W–O and foam-like W–O deposits, were employed. Each one was irradiated with a stripe of NIR pulses and a stripe of UV pulses, on the right-hand side and left-hand side, respectively. Each stripe delivered to the sample an average of 22 pulses per site. The samples were then rotated 90° clockwise, and irradiation with NIR and UV pulses was repeated in the same manner. As shown in figure 5(*a*), this resulted in a mapping of the sample which allowed us to directly evaluate the efficacy of the two wavelengths, taken alone or in combination. Comparing the right-hand side and the left-hand side of the mirror contaminated with compact W–O (figure 5(*b*)), it is evident that the cleaning process yields better results if the samples are treated with UV pulses first. No difference can be observed between the bottom-right corner (UV cleaning first, then NIR) and top-right corner (UV cleaning twice). Considering the mirror with porous W–O contamination (figure 5(*c*)), in the region treated using only NIR pulses (central-left region) the cleaning is not satisfactory, and there is some material left on the mirror surface. When UV pulses are involved the process of contaminant removal is much more effective, and the three other regions (NIR then UV, UV then NIR, and UV twice) look equally clean.

In conclusion, laser cleaning with a UV wavelength seemed definitely a preferable option to that with an NIR wavelength, even if the laser fluence was three times smaller. For this reason we decided to use UV laser light for all the cleaning experiments here reported. Such a sharp variation of the cleaning efficacy depending on the laser wavelength was not observed in the case of carbon contamination [16]. It can be explained considering that W-based contaminants are (to different extents) oxidized, and thus they present an optical band gap which inhibits the absorption of NIR photons (the band gap for crystalline WO_3 is about 2.8 eV, while the photon energy for $\lambda = 1064$ nm is 1.17 eV). This consideration may retain its validity in the general case of dielectric materials with an optical band gap: for that kind of contamination, it would be probably better to perform the laser cleaning with a wavelength short enough to allow inter-band photon absorption.

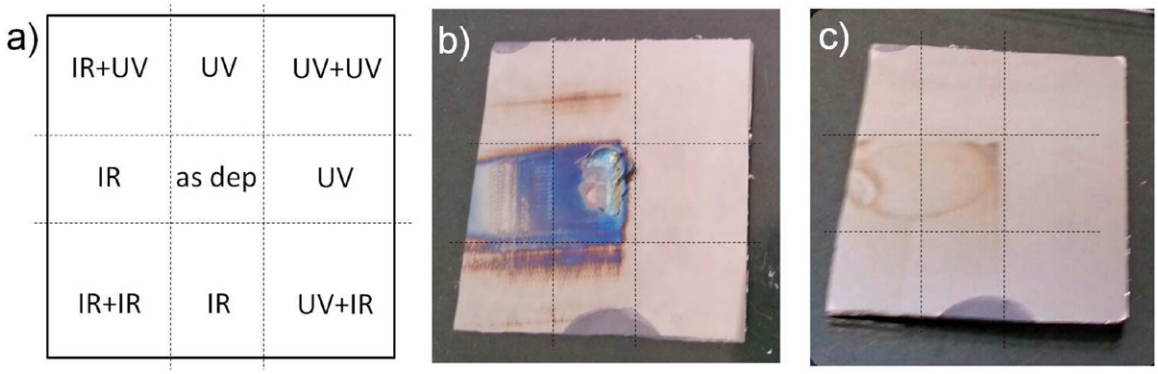

Figure 5. (*a*) Schematic of the laser irradiation pattern. The samples have been rotated by 90° clockwise after the first irradiation and then restored to the original orientation by a 90° counter-clockwise rotation after the second irradiation. (*b*) Compact W–O irradiated with NIR and UV pulses. (*c*) Porous W–O irradiated with NIR and UV pulses. The brown halo in the bottom part of the mirrors is due to the shading effect of the substrate holder during Rh coating deposition.

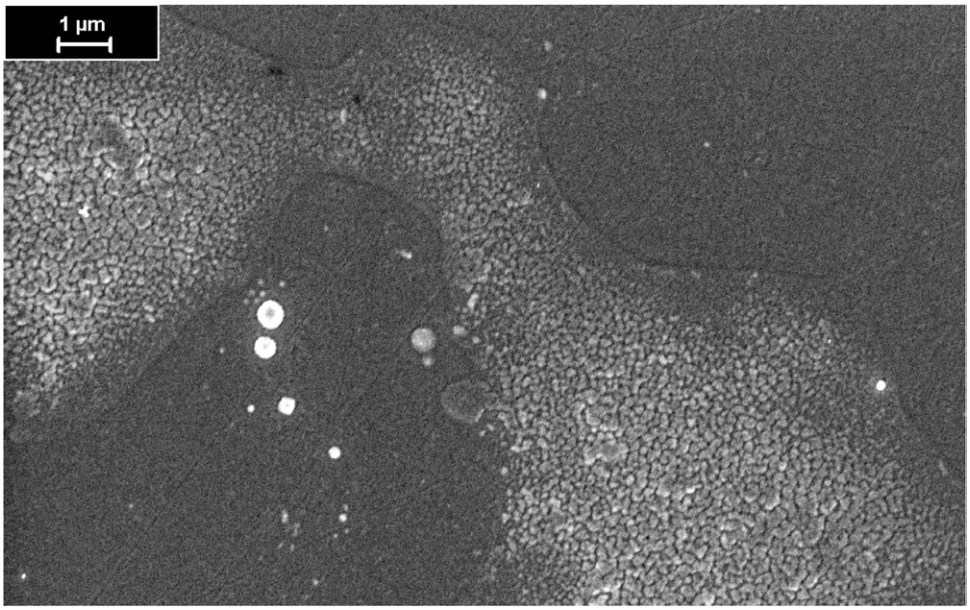

Figure 6. SEM top view of W–O residuals observed after one UV scan on a Rh mirror contaminated with compact W–O.

5. Cleaning results

The most important feature of a diagnostic FM is its specular reflectance R_{spec}. Therefore, the cleaning results are mainly discussed in terms of R_{spec} recovery, i.e. how much the reflectance after the laser cleaning process is close to the original reflectance of an uncontaminated mirror. The surface of the cleaned mirrors was characterized by SEM, to detect possible damage to the Rh film as a consequence of laser irradiation and to investigate the presence of residual materials not removed during the laser cleaning process. The residuals were also characterized by EDXS and Raman spectroscopy.

5.1. Laser cleaning of compact W–O contaminants

A Rh mirror deposited on Si and contaminated with compact W–O was initially cleaned with a single scan. At visual inspection, the sample surface globally recovered the original shiny appearance of metallic Rh, except for a few tiny brown streaks in some areas of the sample. SEM and EDXS analyses revealed that the brown streaks shown in figure 6 are made of oxidized W residuals, with a different morphology from that of the as-deposited contaminant (which was essentially featureless). Raman spectra collected from the brown streaks (not shown) are similar to those from non-irradiated compact W–O, with an increase in the 960 cm^{-1} band intensity. This suggests that the residuals are made of highly-nanostructured tungsten oxide. To remove the streaks, the same sample was cleaned again with an additional scan, using the same parameters of the previous one.

By visual inspection, the sample treated with two scans was indistinguishable from an uncontaminated Rh mirror. While no more well-defined W–O residuals were clearly detectable with SEM, EDXS still revealed traces of W and O on the mirror's surface. The intensity of Raman signals collected from the surface (not shown) was not high enough to be clearly distinguished from noise. No laser-induced damage of the mirror surface was observed.

Figure 7 shows the R_{spec} of a typical Rh mirror as deposited (line I, solid black), contaminated with a compact W–O film

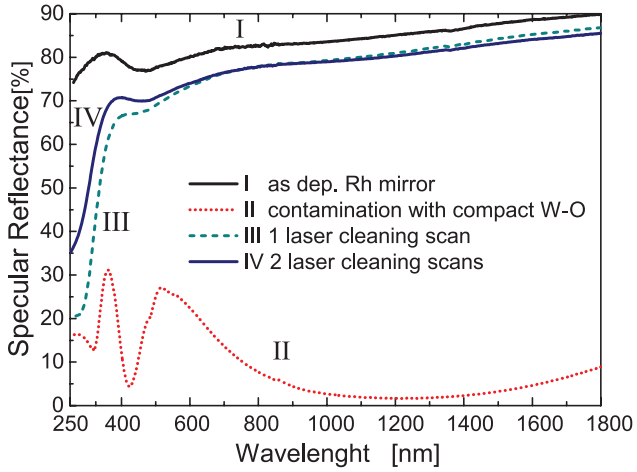

Figure 7. Laser cleaning of Rh mirrors from compact W–O contaminants. R_{spec} of: as dep. Rh mirror (I, solid black); Rh mirror after compact W–O contamination (II, dotted red); Rh mirror after one UV cleaning scan (III, dashed light blue); Rh mirror after two UV scans (IV, solid dark blue).

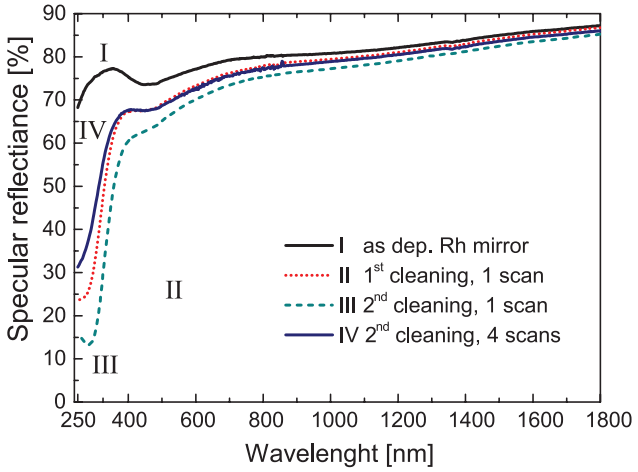

Figure 8. Laser cleaning of Rh mirrors from compact W–O contaminants. R_{spec} of: as dep. Rh mirror (I, solid black); cleaning after first contamination with one UV scan (II, dotted red); cleaning after second contamination with one UV scan (III, dashed light blue); cleaning after second contamination with three additional UV scans (IV, solid dark blue).

(line II, dotted red), after a single UV scan (line III, dashed light blue), and after two scans (line IV, solid dark blue).

Comparing lines I and III, satisfactory R_{spec} recovery is evident in the NIR–vis region (>90% of the pristine value) after the first cleaning scan. For $\lambda < 400$ nm, however, there is a sharp drop of line III. This threshold wavelength is close to the optical band gap of the W–O contaminants (see figure 4 and the related discussion). The inability to recover R_{spec} for $\lambda < 400$ nm can therefore be attributed to the strong UV light absorption by the W–O residuals left on the mirror surface after the laser cleaning scan.

The specular reflectance after two cleaning scans (line IV) is close to line III (one cleaning scan) for $\lambda > 400$ nm, where R_{spec} recovery is already satisfactory. In the UV spectral region the beneficial effect of an additional cleaning cycle is much more evident (R_{spec} has increased by ≈15%). Even though we do not extend the investigation to other scans, it is probable that additional cleaning scans would further improve the UV R_{spec} recovery, in as far as the mirror is not damaged by the laser cleaning process. As a general consideration, if mirrors with a higher laser damage threshold (e.g. polycrystalline mirrors) are used, the range of cleaning parameters (e.g. laser fluence) can be widened, possibly leading to a better cleaning efficacy in the UV region as well.

In a real tokamak environment, each diagnostic mirror may have to be cleaned several times during its life. Therefore, the impact of repeated sequences of contamination and cleaning on mirror performance needs to be addressed. A preliminary assessment of this issue was made by repeating the process of PLD contaminant deposition on a mirror that previously underwent a laser cleaning treatment. To address this issue, another Rh mirror, deposited on P-91 stainless steel, was contaminated with compact W–O. The use of a metallic substrate instead of silicon ensured better adhesion with Rh. In addition, a steel substrate is surely more realistic with respect to the actual FM design in ITER. Since the surface roughness of a polished steel substrate (some nm) is higher than that of

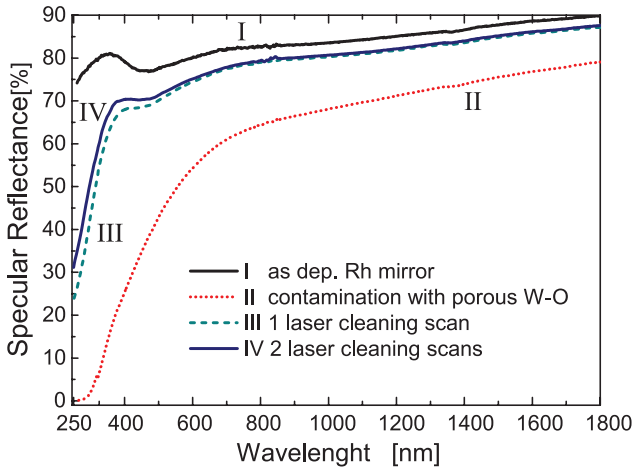

Figure 9. Laser cleaning of Rh mirrors from foam-like W–O contaminants. R_{spec} of: as dep. Rh films (I, solid black); foam-like W–O contaminant (II, dotted red); Rh mirror after one UV scan (III, dashed light blue); Rh mirror after two UV scans (IV, solid dark blue).

Si wafer (∼0.1 nm), the specular component of reflectance is slightly lower (∼5%) for mirrors on stainless steel. Besides this, the properties of the mirrors are not significantly influenced by the nature of the substrate. After a first UV scan with the same parameters described above, mirror reflectance was recorded (figure 8, line II, dotted red). Then, the cleaned mirror was re-deposited with the same kind of compact W–O contaminant. The total, diffuse and specular reflectance of the mirror after the second contamination (not shown) are almost identical to those measured after the first contaminant deposition. The sample was cleaned again, initially with a single UV scan (figure 8, line III, dashed light blue) and then with three additional scans (figure 8, line IV, solid dark blue). By comparing line II and line III, it appears that the R_{spec} recovery ensured by a single scan after two contamination cycles was

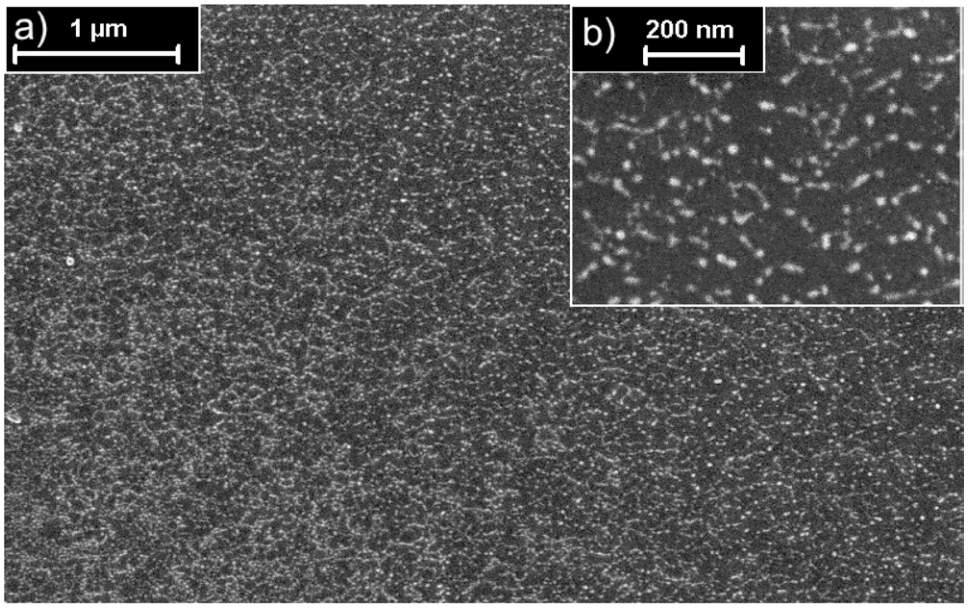

Figure 10. (*a*) SEM top view of the W–O residuals observed after one UV scan on a Rh mirror contaminated with porous W–O. (*b*) High-magnification SEM micrograph where a peculiar rod-shaped morphology of the residuals can be observed.

not as good as the R_{spec} recovery for a single contamination. Nevertheless, the addition of three supplementary cleaning scans (each one followed by a 90° rotation of the sample) enhanced the mirror reflectance significantly, giving an R_{spec} recovery even higher than that achieved for a single contaminant deposition. The Rh film maintained its integrity after the whole process consisting of two contaminant depositions and five cleaning scans.

5.2. Laser cleaning of porous W–O contaminants

A Rh mirror deposited on Si was contaminated with porous W–O and then treated with two cleaning scans. The reflectance was measured after contamination and after each cleaning session, as shown in figure 9. The R_{spec} after the first cleaning scan (line III, dashed light blue) is close (from 90% to 95%) to its pristine values (line I, solid black) in the NIR–vis region, and suffers a sharp decrease for $\lambda < 400$ nm. A second cleaning cycle (line IV, solid dark blue) partially mitigates this issue, ensuring an additional R_{spec} recovery of about 10% in the UV region. Also in this case, the low reflectance in the UV spectrum can be attributed to nanometric residuals left after cleaning. Their peculiar morphology can be observed in figure 10.

Another Rh mirror deposited on a Si substrate was contaminated with foam-like W–O and exploited to study the effect of multiple contamination–cleaning cycles. The procedure was the same as described in the case of compact W–O. The reflectance of the sample was measured after each stage of the process: the first contaminant deposition (figure 11, line II, dotted red), the first cleaning session (line III, dashed light blue), the second contaminant deposition (not shown since it is very close to line II) and the second cleaning session (line IV, solid dark blue). Line III and line IV have the same trend in the cleaning trials described so far, with a good

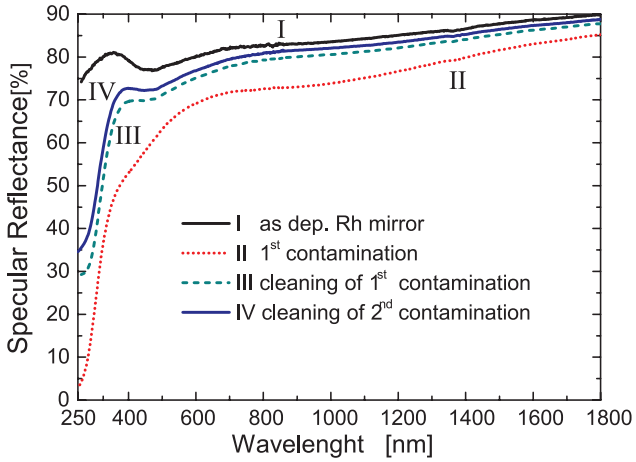

Figure 11. Laser cleaning of Rh mirrors from porous W–O contaminants. R_{spec} of: as dep. Rh films (I, solid black); after first contamination (II, dotted red); after cleaning of first contamination with one UV scan (III, dashed light blue); after cleaning of second contamination with one UV scan (IV, solid dark blue).

reflectance recovery in the NIR–vis region and a marked decrease in the UV region. R_{spec} recovery is slightly better for the second cleaning session, and therefore no additional scans are performed. The Rh film integrity after the whole process was confirmed by both visual and SEM analysis. From this result, one can conclude that the repetition of contamination–cleaning cycles does not seem to worsen the laser cleaning efficacy and the performance of the mirrors, at least for porous W–O contamination in laboratory conditions.

Despite the dramatic differences in their morphology and optical properties, compact and foam-like contaminants showed very similar responses to laser cleaning. It is worth noting that, by comparison, in the case of C-based contamination the deposit morphology plays a major role in determining the laser cleaning outcome, as we reported in [16].

6. Conclusions

This paper presents an experimental investigation of the laser cleaning of diagnostic FMs with laboratory facilities in tokamak-relevant conditions. By means of PLD, Rh films functional as FMs and W-based contaminants with selected properties were produced. The same laser source was exploited to remove the contaminants from the Rh films' surface thanks to the laser cleaning technique. We chose two peculiar morphologies of contaminants, compact W–O and porous foam-like W–O, which can be representative of the re-deposits found in tokamaks or linear plasma devices. By means of a remote handling procedure it was possible to clean relevant areas (some cm^2) in reasonable time (a few minutes). Preliminary cleaning tests showed that UV pulses were more effective than NIR, because of the W–O optical band gap which inhibited NIR photon absorption. Therefore, subsequent cleaning experiments were performed with UV pulses, and the value of the laser fluence per pulse (110 mJ cm^{-2}) was chosen to avoid mirror damaging. As a general remark, we observed that the response to the cleaning process was similar for compact and foam-like W–O, despite the very different morphologies. The specular reflectance was recovered satisfactorily in the NIR and vis spectral ranges ($400\,nm \leqslant \lambda \leqslant 1800$ nm). The rather poor R_{spec} recovery for $\lambda < 400$ nm was attributed to the strong inter-band light absorption by the residuals left on the mirror surface. Additional laser scans beyond the first one seemed to resolve this issue; further experiments are foreseen to determine whether good UV reflectance recovery can be achieved in this way. Considering the laser cleaning of FMs in a real fusion machine, it is expected that multiple cleaning sessions will be necessary during the mirrors' lifetimes. The experiments here presented on mirrors that underwent two consecutive cycles of contamination and cleaning did not show a net degradation in cleaning efficacy. Additional tests with several contamination/cleaning cycles would be useful to confirm the robustness of the laser cleaning technique against repeated depositions of contaminants. Experiments are now ongoing to study different classes of contaminants, such as mixed co-deposits containing a suitable beryllium proxy, also in comparison or together with other cleaning techniques (e.g. plasma cleaning, in collaboration with the University of Basel [7, 9]). In addition, the realization of benchmark laser cleaning tests on mirrors exposed in operating tokamaks would be extremely useful in order to validate the lab-scale approach hereby followed.

Acknowledgments

The authors wish to thank S Perissinotto, V Russo and L Marot for their useful discussions. This project has received funding from the European Union's Horizon 2020 research and innovation programme under grant agreement number 633053. The views and opinions expressed herein do not necessarily reflect those of the European Commission. The research leading to these results has also received funding from the European Research Council Consolidator Grant ENSURE (ERC-2014-CoG No. 647554).

References

[1] Walsh M. *et al* 2011 *IEEE/NPSS 24th Symp. Fusion Engineering (Chicago, 26–30 June 2011)* vol 1 (doi: 10.1109/SOFE.2011.6052210)
[2] Mukhin E.E. *et al* 2012 *Nucl. Fusion* **52** 013017
[3] Litnovsky A. *et al* 2009 *Nucl. Fusion* **49** 075014
[4] Litnovsky A. *et al* 2013 *Nucl. Fusion* **53** 073033
[5] Ivanova D. *et al* 2014 *Phys. Scr. T* **159** 014011
[6] Arkhipov I. *et al* 2013 *J. Nucl. Mater.* **438** S1160
[7] Moser L. *et al* 2015 *Nucl. Fusion* **55** 063020
[8] Razdobarin A.G. *et al* 2015 *Nucl. Fusion* **55** 093022
[9] Moser L. *et al* 2016 *Phys. Scr. T* **167** 014069
[10] Widdowson A. *et al* 2011 *J. Nucl. Mater.* **415** S1199
[11] Zhou Y. *et al* 2011 *J. Nucl. Mater.* **415** S1206
[12] Vatry A., Marchand A., Delaporte P., Grojo D., Grisolia C. and Sentis M. 2011 *Appl. Surf. Sci.* **257** 5384
[13] Skinner C.H., Gentile C.A. and Doerner R. 2013 *Fusion Sci. Tech.* **64** 1
[14] Wisse M. *et al* 2014 *Fusion Eng. Des.* **89** 122
[15] Uccello A., Maffini A., Dellasega D. and Passoni M. 2013 *Fusion Eng. Des.* **88** 1347
[16] Maffini A., Uccello A., Dellasega D., Russo V., Perissinotto S. and Passoni M. 2015 *J. Nucl. Mater.* **463** 944
[17] Passoni M., Dellasega D., Grosso G., Conti C., Ubaldi M.C. and Bottani C.E. 2010 *J. Nucl. Mater.* **404** 1
[18] Uccello A., Dellasega D., Perissinotto S., Lecis N. and Passoni M. 2013 *J. Nucl. Mater.* **432** 261
[19] Eren B. *et al* 2011 *Fusion Eng. Des.* **86** 2593
[20] Brezinsek S. and JET-EFDA Contributors 2015 *J. Nucl. Mater.* **463** 11
[21] Rasinski M. *et al* 2011 *Fusion Eng. Des.* **86** 1753
[22] Kajita S., Sakaguchi W., Ohno N., Yoshida N. and Saeki T. 2009 *Nucl. Fusion* **49** 095005
[23] De Temmerman G. *et al* 2012 *J. Vac. Sci. Technol.* A **30** 041306
[24] Baserga A. *et al* 2012 *Thin Solid Films* **515** 6465
[25] Boulova M. and Lucazeau G. 2002 *J. Solid State Chem.* **167** 425
[26] Bennett H.E. and Porteus J.O. 1961 *J. Opt. Soc. Am.* **51** 123